Short Communication

Influence of Zirconium Content on Corrosion Resistance of Micro-Alloyed Steel Reinforced Concrete in Chloride Solutions

Shi Shao Hua

School of Architectural Engineering Sichuan University of Arts and Science, Dazhou,
Sichuan Province, 635000, China
E-mail: sshssh080612@sina.com

Corrosion resistance of zirconium(Zr) micro-alloyed steel rebar in the artificial seawater environment were investigated by electrochemical technique. Electrochemical impedance spectroscopy (EIS) and potentiodynamic polarization techniques were used to study the effect of Zr content on corrosion behavior of carbon steel rebars.The polarization plots show that the steel rebar with 0.15 wt% Zr content had a smaller corrosion current-density than the other samples which was in the passive state during the test.The EIS results indicate that double-layer capacitance value is reduced with the increase ofZr content which reveals that the passive film thickness increased resulting in an enhanced protective capacity when the Zr content of steel rebar gradually increased. The EIS results are in accordance with the best-fit findings for double-layer capacitance at the steel–concrete interface which were gradually increased over 4.5 µFcm^{-2} with 3 wt% NaCl in the artificial seawater, demonstrating that produced corrosion may occur on the surface of steel rebar.

1. INTRODUCTION

A large number of literature has been generated by researchers based on the research studies conducted by them on the occurrence of corrosion and protection of steel rebar reinforced concrete [1]. This is mainly due to the significance of the steel-reinforced concrete as a predominantly used construction material. Corrosion of the steel reinforcement affects the durability of the concrete structures which occurs due to the influence of Chlorine (Cl$^-$) ions into the concrete matrix [2, 3]. To prevent this influence and to rectify the after effects, researchers have been developing many electrochemical treatments for the last 25 years. Some patented works have been considered as a rule and are being applied to many construction works. Thus, the suitable and efficient methods that are

commonly accepted to enhance the durability of the concrete are both cathodic protection and electrochemical chloride extraction [4, 5].

Numerous corrosion resistant rebars have previously been manufactured and used in the reinforced concrete at an aggressive environment, for example stainless steel rebar and epoxy-coated rebar [6, 7]. However, due to the high cost of construction and production, these rebars are still used only in extremely aggressive environments. Recent studies showedthat micro-alloyed steel rebar can be evaluated in an aggressive environment [8-10]. By adding one or more anti-corrosion alloy elements, such as molybdenum, chromium, aluminum, nickel, copper and silicon, the corrosion resistance of steel rebar can be improved in comparison with the general carbon steel rebar [11-13]. However, due to the low amount of alloying element used, the cost of production can be significantly reduced.Consequently, this alloyed rebar has great potential that can be used as a replacement for the carbon steel bars with a much longer service life in an aggressive environment [14, 15]. Electrochemical impedance spectroscopy (EIS) method as a sensitive nondestructive instrument can be applied to consider the microstructure, physical, mechanical and electrical properties of the reinforced concrete [16-18]. To describe the concrete-steel system, the EIS method has also made it possible to study the corrosion phenomenon of steel.

Many researches have been focusing on the study of alloying elements effect on corrosion of steel rebars in corrosive environments [19-21]. However, the studies in the zirconium (Zr) content on steel rebar by the electrochemical process have not been published yet. Therefore, in this work, the effect of Zr content on steel rebar corrosion in an artificial seawaterwere investigated. The electrochemical impedance spectroscopy and potentiodynamic polarization techniques were utilized to study the electrochemical properties of Zr micro-alloyed carbon steel rebar.

2. MATERIALS AND METHOD

100 mm long cylindrical concrete samples with a width of 50 mm and a 10 mm diameter steel rod embedded in their centers were made. Chemical cleaning was done on the steel surface before using. The chemical composites of the four kinds of low-carbon steel rebars are listed in Table 1. Table 2 presents the chemical composition of the common Portland cement used. Cardboard molds were used to form the specimens and then placed in a room at 20 ℃ with no humidity for a day.

Table 1. Chemical compositions of Zrmicroalloyed low-carbon steel rebars (wt%)

Alloys	Fe	C	Mn	Si	P	S	Zr
Zr-0.0 wt%	Residual	0.25	1.55	0.50	0.03	0.025	0.0
Zr-0.05 wt%	Residual	0.24	1.55	0.53	0.03	0.025	0.05
Zr-0.1 wt%	Residual	0.24	1.55	0.50	0.03	0.025	0.1
Zr-0.15 wt%	Residual	0.24	1.55	0.50	0.03	0.025	0.15

Table 2. Chemical composition of the Portland cement

Compositions	Contents (wt%)
CaO	62.8
SiO$_2$	21.8
Al$_2$O$_3$	4.7
Fe$_2$O$_3$	2
MgO	2
SO$_3$	3.8
LoI	1.8

After removing the mold, the samples were kept in a wet room at 20 ± 1 °C and 100% relative humidity for 28 days and then exposed to contact with artificial seawater solution for the first time.

Electrochemical impedance spectroscopy (EIS) experiments were performed with a model EA-201 Electro Analyzer (chemilink systems), equipped with a personal computer that was used for electrochemical measurement and treating of data. A conventional three-electrode cell was employed throughout the experiments, with steel reinforced concrete as a working electrode, a saturated calomel electrode as a reference electrode, and a platinum electrode as a counter electrode. EIS characterizations were done at the frequency varied between 100 kHz and 10 mHz at the applied AC amplitude of 10 mV. All electrochemical measurements were done in 1000 ml of an artificial seawater, which is believed to be the representative of the corrosive environment. Each litter of artificial seawater contained 36.0 g of a commercially available artificial salt mix with the following composition (gl^{-1}) [22]: 24.53 NaCl, 4.09 Na$_2$SO$_4$, 5.20 MgCl$_2$, 1.16 CaCl, 0.025 SrCl$_2$, 0.695 KCl, 0.201 NaHCO$_3$, 0.101 KBr, 0.027 H$_3$BO$_3$, and 0.003 NaF. The pH of the artificial seawater medium was about 7.7 ±0.1 and was then adjusted to 7.5 using a 0.1 M hydrochloric acid solution. Furthermore, for evaluating Cl$^-$ ion concentration effect on corrosion behavior, the experimental was performed in different concentrations of NaCl solution (0, 1, 2 and 3 wt%). The morphologies of the samples were done by scanning electron microscope (SEM, FEI/Nova NanoSEM 450). The potentiodynamic polarization (CorrTest Instruments Corp., Ltd., China) measurement was conducted from 0.25V at 1 mV/s scanning rate.

3. RESULTS AND DISCUSSION

Potentiodynamic polarization method is a conventional electrochemical technique to determine corrosion rate of the samples. From polarization plots in Figure 1, sample D (0.15 wt% Zr content) shows noticeable passivation in the solution and the most positive in pitting potential.

According to the Tafel extrapolation method [23], the corrosion parameters of the steel samples were obtained by fitting the polarization curves, using the Corrview software. Tafel extrapolation is a well-known method. When the value of the applied potential is far enough away from the corrosion potential, the polarization curve only reflects the kinetics information of one electrode process in the anodic or cathodic branch. Therefore, the linear parts of the polarization curve can be extrapolated into

an intersection, which provides the values of E_{corr} and i_{corr}[24]. The value of parameters is summarized in Table 3.
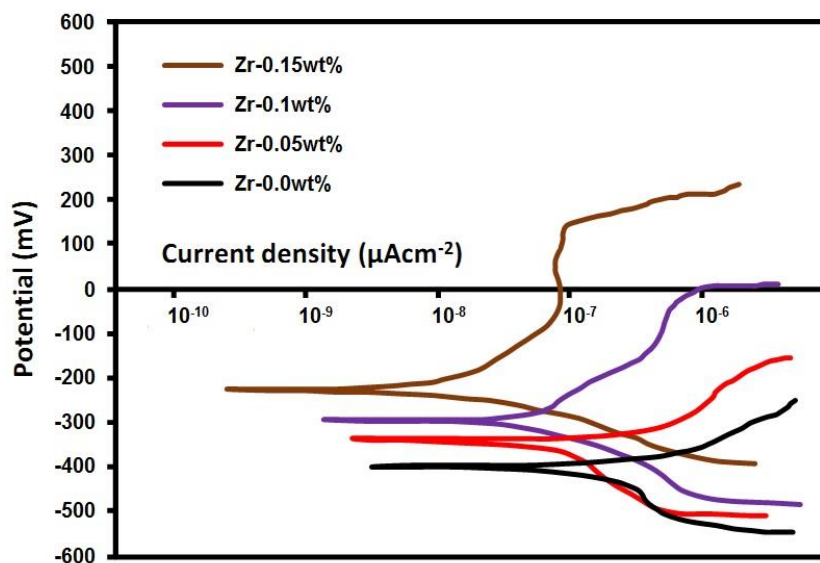

Figure 1. Polarization plots of the samples with different Zr content exposed to the artificial seawaterat 1 mV/s scanning rate and 25 °C temperature.

Table 3. Fitting parameters of the samples obtained from polarization plots in an artificial seawater at 25 °C temperature.

Alloy	Corrosion current density (μAcm^{-2})	Corrosion potential (mV)	β_c (mVdec^{-1})	β_c (mVdec^{-1})
Zr-0.0 wt%	0.827	-415	45	87
Zr-0.05 wt%	0.543	-345	52	94
Zr-0.1 wt%	0.096	-298	63	91
Zr-0.15 wt%	0.045	-223	77	88

The corrosion level can be defined into four levels proposed by Durar Network Specification [25]: very high corrosion for 1.0 $\mu A/cm^2 < i_{corr}$, high corrosion for 0.5 $\mu A/cm^2 < i_{corr} < 1.0$ $\mu A/cm^2$, low corrosion for 0.1 $\mu A/cm^2 < i_{corr} < 0.5$ $\mu A/cm^2$, and passivity for $i_{corr} < 0.1$ $\mu A/cm^2$. According to Table 2, the steel rebar with 0.15wt% Zr content had a smaller corrosion-current density than the other samples which was in the passive state during the test.

The E_{corr} of the 0.15 wt% Zr sample was considerably shifted to a more positive value in comparison with the other samples, which shows that the self-corrosion potential was enhanced after the addition of Zr. Moreover, the cathodic plots of the specimens shifted downwards as the Zr content increased, which revealed that the rates of cathode reaction at this stage were relatively low [26]. Furthermore, cathodic Tafel slope (β_c) and anodic Tafel slope (β_a) as well as the i_{corr} were calculated by the Tafel extrapolation technique. As shown in table 3, β_c and β_a values were changing with the change in the Zr concentration. The changes in the values of Tafel slope can be utilised to recognise the

inhibition mechanism (cathodic oranodic) for carbon steel, the electrolyteconcentration, the charge transfer coefficient and the working electrode composition [27].The values of the β_c significantly unchanged with the increase of Zr, which suggests that its cathodic reaction influence did not improve the hydrogen evolution discharge mechanism [28, 29]. However, the slope values of the anodic Tafel changed significantly with the Zr addition suggesting that there were blockage at the sites of anodic reaction, and thus affect themechanism of anodic reaction. Moreover, with the increase of alloying element Zr, the anode Tafel slope increased which means that Zr element can promote a corrosion protection of carbon steel rebars in the artificial seawater.
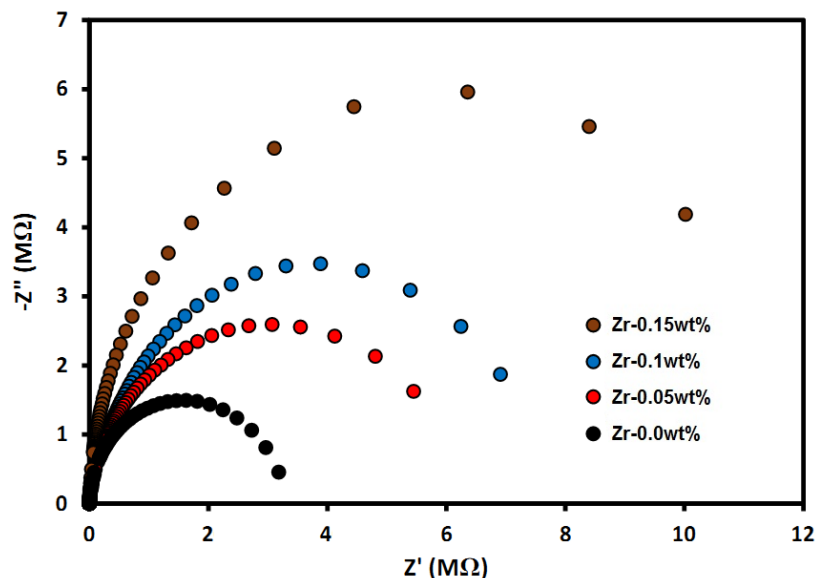

Figure 2. Nyquist diagram of the samples with different Zr content exposed to the artificial seawaterat the applied AC amplitude of 10 mV and 25 °C temperature.

EIS technique has been extensively employed in the analysis of the passive layer of rebars due to its capability to characterize redox reactions of steel rebars in an alkaline environment[30]. EIS was conducted to analyze the effect of Zr micro-alloy amount on the corrosion behavior of rebars with passive layers in the artificial seawater. Figure 3 indicates an equivalent circuit with two times constants which suggested to simulate the electrochemical procedure of steel rebars used by other researchers. R_m is the mortar resistance which correspond to the high-frequency response[31]. Since, the resistance of electrolyte was insignificant compared to the resistance of mortar in this study, the electrolyte resistance was therefore neglected.During the passivity process, the parameters of second time constant observed at the low frequencies such as R2 and C2 were ascribed to the charge transfer resistance and non-ideal interfacial capacitance of the steel surface. It indicatedthat the corrosion protection of the steel rebar was controlled by the passive film properties [32-34]. The parameters of first time constant observed at the low frequencies such as R_1 and C_1 were attributed to the redox transformation in the corrosion products which happened on the oxide film surface.
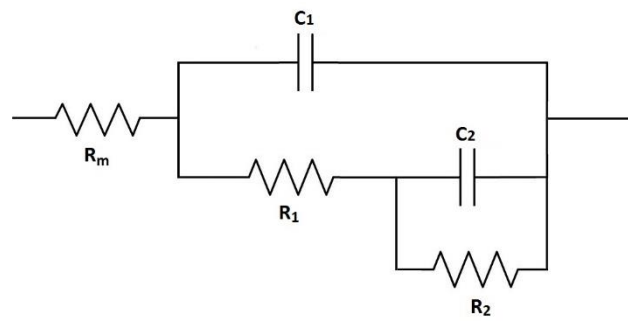
Figure 3. An equivalent circuit model to fit the experimental data

Polarization resistance, R_p ($R_p = R_1 + R_2$) is a computable indicator to consider the steel corrosion resistance in the corrosive environment. So that the higher R_p value indicates higher corrosion resistance of the sample.

Table 4. Electrochemical parameters from the fitting using the equivalent circuit in an artificial seawater at 25 °C

Alloy	R_m (Ω cm^2)	R_1(MΩ cm^2)	C_1(μF cm^{-2})	R_2 (MΩ cm^2)	C_2 (μF cm^{-2})
Zr-0.0 wt%	54.6	1.96	3.4	3.42	4.3
Zr-0.05 wt%	63.2	3.17	3.1	6.31	3.8
Zr-0.1 wt%	58.4	4.26	2.6	7.95	3.2
Zr-0.15 wt%	72.7	6.85	2.2	12.46	2.8

According to table 4, increasing the Zr contents show a significantly enhancement in R_p value indicating a higher corrosion resistance for 0.15 wt% Zr steel rebar.

Figure 4 indicates the SEM images of samples after exposed to the artificial seawater for 4 weeks. Extensive corrosion occurs on the surface of samples with 0 wt% and 0.05 wt% Zr, demonstrating the high corrosion state. Furthermore, few small pits appears on the surface of sample with 0.1 wt% Zr, and the surface of sample with 0.15 wt% Zr was clean and smooth without any visible corrosion zones, which means the samples with 0.1 wt% and 0.15 wt% Zr have a suitable corrosion resistance even in an aggressive environment. These findings reveal that the addition of Zr element enhances the corrosion resistance which is in agreement with the results of the electrochemical measurements.
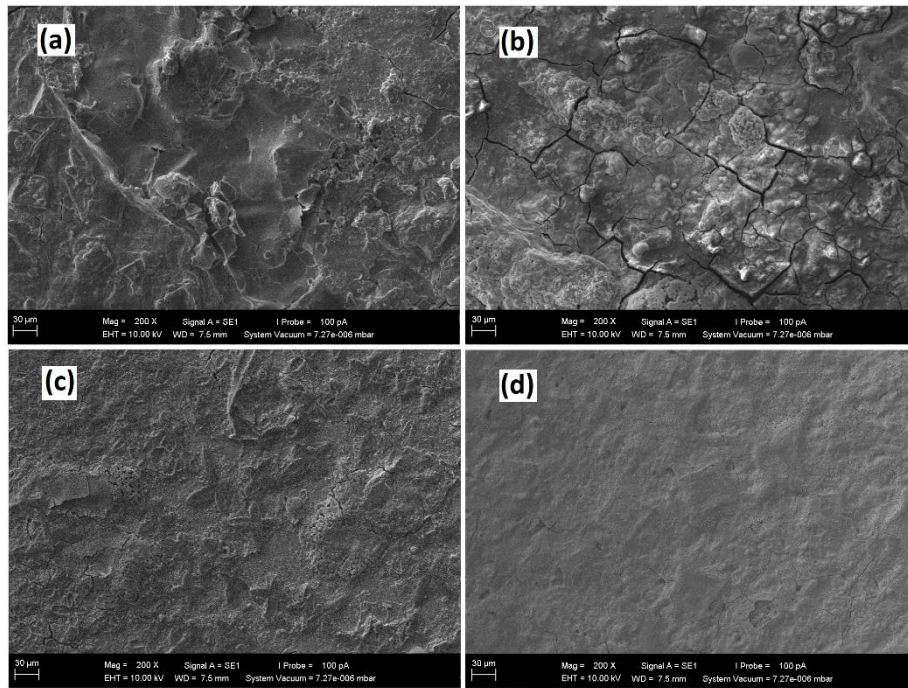
Figure 4. SEM images of the samples with different content of Zr, (a) 0 wt% (b) 0.05 wt% (c) 0.1 wt% (d) 0.15 wt% in an artificial seawater at 25 °C temperature.
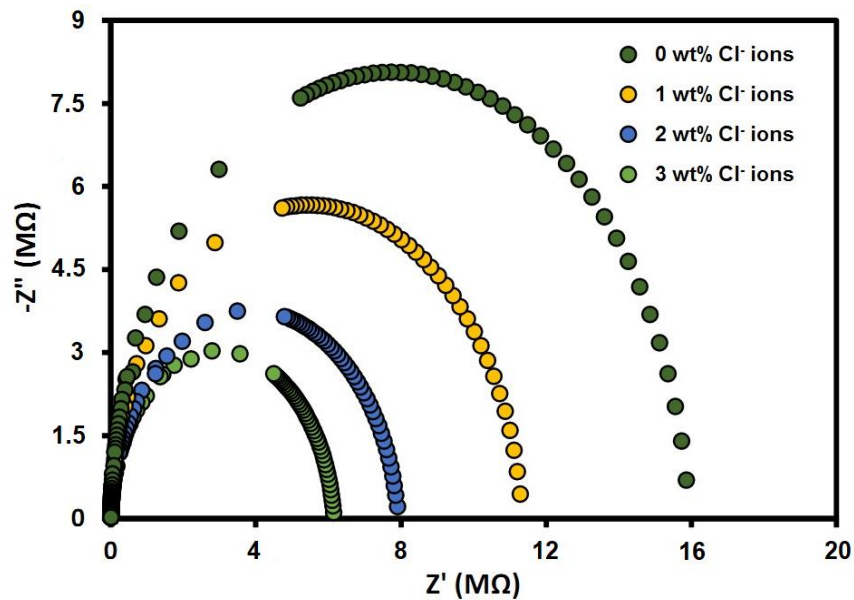

Figure 5. EIS diagrams of the steel rebar with 0.15 wt% Zr immersed into the electrolyte solution with different concentration of Cl⁻ ions at the applied AC amplitude of 10 mV and 25 °C temperature.

The Nyquist diagrams of EIS obtained in artificial seawater with various concentrations of chloride (Cl⁻) ions is shown in Figure 5. Nyquist plots typically indicate a capacitive loop which the diameter of the loops were reducing with increase of Cl⁻ ions. It can be attributed to the corrosion

behavior of Cl⁻ ions on the surface of steel. The EIS plot at the high-frequency proposes the resistance between the working electrode and the electrolyte solution.

Moreover, the EIS diagram at the low-frequency can be associated to the charge transfer resistance in the corrosion procedure [35].

The best fittingelements based on the electrical circuit revealed in figure 3 are listed in Table 5. As shown, the R_2 value is significantly reduced from 16.1 MΩ to 6.23 MΩ, by adding a small amount of NaCl in the electrolyte solution, indicating that the presence of Cl⁻ ions had led to an enhanced corrosion on the steel surface.

Table 5. Electrochemical parameters from the fitting using the equivalent circuit in Figure 3 for different concentration of Cl⁻ ions at 25 °C temperature.

Concentration ofCl⁻ ions	R_m (Ω cm²)55555	R_1(MΩ cm²)	C_1(μF cm⁻²)	R_2 (MΩ cm²)	C_2 (μF cm⁻²)
0 wt%	46.4	9.12	1.7	16.1	2.2
1 wt%	44.5	7.33	2.4	11.42	2.9
2 wt%	53.8	5.26	3.1	8.01	3.6
3 wt%	43.2	3.21	3.8	6.23	4.5

Furthermore, table 5 indicates that R_1 gradually decreased by increasing the chloride concentration which shows that non-protective corrosion and porous products had been advanced on thesurface of steel rebar. These results are in accordance with the best-fit findings for C_2 which were steadily increased over 4.5 μFcm⁻² with 3 wt% Cl⁻ ions in the electrolyte solution, demonstrating that generalized corrosion may occur on the surface of the steel rebar [36].

4. CONCLUSIONS

In this research, carbon steel reinforced concrete were used to study the corrosion behavior of Zr micro-alloyed steel rebar in the artificial seawater. SEM images indicate that the surface of steel rebar with 0.15 wt% Zr was clean and smooth without any visible corrosion zones, which means the 0.15 wt% Zr sample has a suitable corrosion resistance even in an aggressive environment. According to polarization plots, the steel rebar with 0.15 wt% Zr content had a smaller i_{corr} than the other samples which was in the passive state during the test. The EIS results indicate that the increase in Zr content leads to an increase in the radius of the capacitive loop which indicates an enhancement of the corrosion resistance for a steel rebar. The EIS results are in accordance with the best-fit findings for double-layer capacitance at the steel–concrete interface which were gradually increased over 4.5 μFcm⁻² with 3 wt% NaCl in the artificial seawater, demonstrating that produced corrosion may occur on the surface of steel rebar.

References

1. A. James, E. Bazarchi, A.A. Chiniforush, P.P. Aghdam, M.R. Hosseini, A. Akbarnezhad, I. Martek and F. Ghodoosi, *Construction and Building Materials*, 224(2019)1026.
2. A. Watanabe, H. Furukawa, S. Miyamoto and H. Minagawa, *Construction and Building Materials*, 196(2019)95.
3. H. Chen, S. Zhang, Z. Zhao, M. Liu and Q. Zhang, *Progress in Chemistry*, 31(2019)571.
4. J. Xu and F. Li, *Ocean Engineering*, 179(2019)38.
5. D. Yuan, C. Zhang, S. Tang, X. Li, J. Tang, Y. Rao, Z. Wang and Q. Zhang, *Water research*, 163(2019)114861.
6. Y.-Z. Mao, Y.-H. Wei, H.-T. Zhao, C.-X. Lv, H.-J. Cao and J. Li, *Acta Metallurgica Sinica (English Letters)*, 31(2018)1171.
7. S. Tang, N. Li, D. Yuan, J. Tang, X. Li, C. Zhang and Y. Rao, *Chemosphere*, 234(2019)658.
8. C. Wu, B. Jia and S. Han, *Journal of Materials Engineering and Performance*, 28(2019)938.
9. D. Song, W. Sun, J.-y. Jiang, H. Ma, J.-c. Zhang and Z.-j. Cheng, *Journal of Iron and Steel Research International*, 23(2016)
10. P. Shao, J. Tian, F. Yang, X. Duan, S. Gao, W. Shi, X. Luo, F. Cui, S. Luo and S. Wang, *Advanced Functional Materials*, 28(2018)1705295.
11. Z. Wang, H. Zhang, C. Guo, W. Liu, Z. Yang, X. Sun, Z. Zhang and F. Jiang, *Journal of materials science*, 51(2016)4996.
12. Y. Tian, M. Liu, X. Cheng, C. Dong, G. Wang and X. Li, *Cement and Concrete Composites*, 97(2019)190.
13. P. Shao, J. Tian, X. Duan, Y. Yang, W. Shi, X. Luo, F. Cui, S. Luo and S. Wang, *Chemical Engineering Journal*, 359(2019)79.
14. V. Sharma and A. Shahi, *Journal of Materials Processing Technology*, 253(2018)2.
15. X. He, F. Deng, T. Shen, L. Yang, D. Chen, J. Luo, X. Luo, X. Min and F. Wang, *Journal of colloid and interface science*, 539(2019)223.
16. S. Zhang, X. Cheng, L. Su and C. Jiang, *International Journal of Electrochemical Science*, 12(2017)2453.
17. P. Shao, L. Ding, J. Luo, Y. Luo, D. You, Q. Zhang and X. Luo, *ACS applied materials & interfaces*, 11(2019)29736.
18. F. Husairi, J. Rouhi, K. Eswar, A. Zainurul, M. Rusop and S. Abdullah, *Applied Physics A*, 116(2014)2119.
19. M. Liu, X. Cheng, X. Li, J. Hu, Y. Pan and Z. Jin, *Case Studies in Construction Materials*, 5(2016)87.
20. M. Liu, X. Cheng, X. Li, P. Yue and J. Li, *Journal of Materials Engineering and Performance*, 25(2016)4967.
21. F.A. Cedrim, V.L.S.d. Almeida, C.A.C.d. Souza, P.R.L. Lima, M.D.d. Jesus and D.V. Ribeiro, *Materials Research*, 22(2019)1.
22. L. Shan, Y. Wang, J. Li, H. Li, X. Wu and J. Chen, *Surface and Coatings Technology*, 226(2013)40.
23. Y. Xu, C. Zhu, S. Chen, Y. Zhang, T. Wu, X. Lu, M. Wang and X. Feng, *International Journal of Electrochemical Science*, 14(2019)9726.
24. S. Zhang, Z. Li, X. Su and C. Yang, *International Journal of Electrochemical Science*, 14(2019)10888.
25. R. Galván-Martínez, C. Gaona-Tiburcio and F. Almeraya-Calderón, *International Journal of Electrochemical Science*, 11(2016)2994.
26. P. Shao, X. Duan, J. Xu, J. Tian, W. Shi, S. Gao, M. Xu, F. Cui and S. Wang, *Journal of hazardous materials*, 322(2017)532.
27. Y. Zhou, S. Xu, L. Guo, S. Zhang, H. Lu, Y. Gong and F. Gao, *RSC Advances*, 5(2015)14804.

28. A. Ansari, M. Znini, I. Hamdani, L. Majidi, A. Bouyanzer and B. Hammouti, *Journal of Materials and Environmental Science*, 5(2014)81.
29. S. Kakooei, H.M. Akil, A. Dolati and J. Rouhi, *Construction and Building Materials*, 35(2012)564.
30. L. Yang, G. Yi, Y. Hou, H. Cheng, X. Luo, S.G. Pavlostathis, S. Luo and A. Wang, *Biosensors and Bioelectronics*, 141(2019)111444.
31. N. Naderi, M. Hashim and J. Rouhi, *International Journal of Electrochemical Science*, 7(2012)8481.
32. H.-S. Ryu, J.K. Singh, H.-S. Lee, M.A. Ismail and W.-J. Park, *Construction and Building Materials*, 133(2017)387.
33. C. Li, S. Hu, L. Yang, J. Fan, Z. Yao, Y. Zhang, G. Shao and J. Hu, *Chemistry–An Asian Journal*, 10(2015)2733.
34. M. Husairi, J. Rouhi, K. Alvin, Z. Atikah, M. Rusop and S. Abdullah, *Semiconductor Science and Technology*, 29(2014)075015.
35. J. Rouhi, S. Kakooei, M.C. Ismail, R. Karimzadeh and M.R. Mahmood, *International Journal of Electrochemical Science*, 12(2017)9933.
36. K. Tang, *Corrosion Science*, 152(2019)153.